Segregated Fronto-Cerebellar Circuits Revealed by Intrinsic Functional Connectivity

Cerebral Cortex October 2009;19:2485–2497
doi:10.1093/cercor/bhp135
Advance Access publication July 10, 2009

Segregated Fronto-Cerebellar Circuits Revealed by Intrinsic Functional Connectivity

Fenna M. Krienen[1,2] and Randy L. Buckner[1,2,3,4]

[1]Department of Psychology, Center for Brain Science, Harvard University, Cambridge, MA 02138, USA, [2]Athinoula A. Martinos Center, Massachusetts General Hospital, USA, [3]Departments of Psychiatry and Radiology, Massachusetts General Hospital, USA and [4]Howard Hughes Medical Institute, USA

Multiple, segregated fronto-cerebellar circuits have been characterized in nonhuman primates using transneuronal tracing techniques including those that target prefrontal areas. Here, we used functional connectivity MRI (fcMRI) in humans ($n = 40$) to identify 4 topographically distinct fronto-cerebellar circuits that target 1) motor cortex, 2) dorsolateral prefrontal cortex, 3) medial prefrontal cortex, and 4) anterior prefrontal cortex. All 4 circuits were replicated and dissociated in an independent data set ($n = 40$). Direct comparison of right- and left-seeded frontal regions revealed contralateral lateralization in the cerebellum for each of the segregated circuits. The presence of circuits that involve prefrontal regions confirms that the cerebellum participates in networks important to cognition including a specific fronto-cerebellar circuit that interacts with the default network. Overall, the extent of the cerebellum associated with prefrontal cortex included a large portion of the posterior hemispheres consistent with a prominent role of the cerebellum in nonmotor functions. We conclude by providing a provisional map of the topography of the cerebellum based on functional correlations with the frontal cortex.

Keywords: cerebellum, cognition, fMRI, pontine nucleus, prefrontal cortex, thalamus

Introduction

The identification of multiple, segregated fronto-cerebellar circuits using viral tracing techniques in nonhuman primates has challenged the traditional view that motor control comprises the complete repertoire of the cerebellum (Middleton and Strick 1994, 2001; Kelly and Strick 2003; see also Leiner et al. 1986; Schmahmann 1991). The presentation of cerebellar patients with cognitive deficits in the absence of motor deficits similarly suggests cerebellar involvement in nonmotor functions (Schmahmann 2004; Schmahmann et al. 2007). Neuroimaging studies finding cerebellar activation in response to nonmotor components of cognitive tasks have complemented this view (Petersen et al. 1989; Allen et al. 1997; Desmond and Fiez 1998; O'Reilly et al. 2008; Stoodley and Schmahmann 2009).

However, there has been no adequate technique to explore fronto-cerebellar circuits in humans. Characterizing such circuits would provide strong evidence of the anatomical substrate of cerebellar contributions to cognition as well as provide a mapping of cerebellar regions as a foundation for further analysis. Of particular interest are the posterior lobes of the cerebellum that are markedly expanded in apes and humans relative to other mammals (MacLeod et al. 2003). The posterior lobes, which include the major extent of the lateral hemispheres, are predicted to project to association areas of cortex and largely spare regions directly involved in motor function.

Functional connectivity based on intrinsic activity fluctuations provides a potentially powerful method for mapping fronto-cerebellar circuits (Biswal et al. 1995; see Fox and Raichle 2007 for a review). Intrinsic fluctuations detected by fMRI are constrained by anatomic pathways such that connected brain regions show correlated fluctuations (Vincent et al. 2007; Johnston et al. 2008). Analysis of functional correlations, often referred to as functional connectivity MRI (fcMRI) analysis, has been used to map multiple brain systems linked to sensory, motor, and cognitive functions (e.g., Biswal et al. 1995; Greicius et al. 2003; De Luca et al. 2006; Fox et al. 2006; Vincent et al. 2006, 2008; Dosenbach et al. 2007; Margulies et al. 2007; Kahn et al. 2008; Zhang et al. 2008). There are strengths and limitations to this technique.

Emerging evidence suggests that fcMRI reflects both monosynaptic and polysynaptic connections (Greicius et al. 2009; Honey et al. 2009). Sensitivity to indirect connectivity presents an opportunity for mapping fronto-cerebellar circuits because the cerebral cortex is anatomically connected to the cerebellum only through polysynaptic projections via the pons or thalamus (Schmahmann 1996; Middleton and Strick 2001; Kelly and Strick 2003). However, sensitivity to indirect connections and the fact that fcMRI reflects correlation rather than direct anatomic projections also limits the specificity of the method (see Buckner et al. 2009 for discussion). For example, fcMRI does not permit recovery of information about the directionality of connections. Also, fcMRI results can lead to ambiguous interpretations of the specific structure of connectivity. When 3 regions show correlated fluctuations, it is not possible to know whether they are all connected or whether 2 regions show correlation mediated by their common connections to the third region. Despite these limitations, the method is particularly useful for identifying segregated pathways. Work on the cingulate (Margulies et al. 2007) and the medial temporal lobe memory system (Kahn et al. 2008) provides examples where segregated brain pathways have been successfully characterized.

Here, we use fcMRI to provide a detailed analysis of fronto-cerebellar circuits, taking advantage of the method's ability to identify segregated pathways. Several prior studies have noted fluctuations in the cerebellum that correlate with the cerebral cortex (e.g., Allen et al. 2005; Fransson 2005; Vincent et al. 2008). Allen et al. (2005) demonstrated the feasibility of using fcMRI to study the functional connectivity between the cerebral cortex and the cerebellar cortex (including the dentate nucleus) in humans, and provided evidence that fcMRI is sensitive to the anatomical constraints governing cerebro-cerebellar connectivity.

The present work expands upon these observations and provides a provisional map of cerebellar topography based on correlations with frontal cortex. The full extent of the cerebellum and cerebral cortex was imaged across 2 independent data sets (each $n = 40$) to systematically map connectivity by seeding multiple frontal regions and exploring correlations in the cerebellum. We first sought to determine whether correlations between the frontal cortex and cerebellum are consistent with established circuit properties observed in nonhuman primates. Studies in the monkey demonstrate that cortical areas project to the contralateral cerebellum via efferents that cross hemispheres between the pons and the cerebellar cortex and afferents between the deep cerebellar nuclei and the thalamus. Furthermore, certain fronto-cerebellar connections are organized as closed, independent circuits, wherein neocortical areas receive input from the very same cerebellar regions that they project to (Middleton and Strick 2000). This connectional architecture, unlike projections between neocortical areas that show convergence and divergence, is ideally structured to test the specificity of fcMRI. Thus, the monkey anatomy suggests there should exist multiple, parallel polysynaptic circuits between frontal cortex and the cerebellum and also that these circuits should exhibit crossed laterality. Once we established that fcMRI recovers known circuit properties of fronto-cerebellar projections, we applied the technique iteratively to map the topography of multiple, segregated circuits between prefrontal cortex and the cerebellum.

Materials and Methods

Participants

Eighty young adults participated for payment (ages 18–28, mean age = 21.5 years, 35 male). All had normal or corrected-to-normal vision and were right-handed, native speakers of English with no reported history of a neurologic or psychiatric condition. Participants provided written informed consent in accordance with guidelines set by institutional review board of Partners Healthcare.

Data Acquisition

Scanning was conducted on a 3T TimTrio scanner (Siemens, Erlangen, Germany) using a 12-channel phased-array head coil. The functional imaging data were acquired using a gradient-echo echo-planar (EPI) sequence sensitive to blood oxygenation level–dependent (BOLD) contrast (time repetition, TR = 3000 ms; time echo, TE = 30 ms; flip angle, FA = 90°; 3 × 3 × 3 mm voxels; 0.5-mm gap between slices; field of view, FOV = 256; interleaved acquisition). Whole-brain coverage including the entire cerebellum was achieved with 43 slices aligned to the anterior–posterior commissure plane. Structural data included a high-resolution T1-weighted magnetization-prepared gradient-echo image (MP-RAGE) (TR = 2530 ms; TE = 3.44 ms; FA = 7°; 1.0-mm isotropic voxels; FOV 256 ×256). Head motion was minimized by using a pillow and padded clamps, and earplugs were used to attenuate noise.

Two separate data sets were collected ("Data Set 1": $n = 40$; "Data Set 2": $n = 40$). Data Set 1 was used to identify, in an exploratory manner, the regions of frontal cortex that correlate with regions in the cerebellum. Data Set 2 was used to formally test for dissociation among fronto-cerebellar circuits generated from the findings in Data Set 1. During all runs of Data Set 1, participants engaged in a passive task state that was either 1) eyes closed rest, 2) eyes open fixating a visual crosshair, or 3) eyes open without fixating. These rest-state variants show minimal differences in functional connectivity (Van Dijk et al. 2008) so, in order to optimize signal to noise, all variants were used when available. Between 2 ($n = 11$) and 6 ($n = 28$) runs of 104 timepoints were collected from each participant. For participants with 6 runs, 2 of each passive task variants were acquired. For participants with 2 runs, only visual fixation was acquired. One participant completed 4 runs of eyes closed rest. Participants completed various tasks unrelated to the present study before the rest runs analyzed here. The visual crosshair was generated on an Apple MacBook Pro (Apple Computer Inc., Cupertino, CA) using Matlab software (The Mathworks, Inc., Natick, MA) and the Psychophysics Toolbox extension (Brainard 1997) and projected onto a screen positioned at the head of the magnet bore. Participants viewed the screen though a mirror attached to the head coil. In Data Set 2, 2 runs were collected from each participant. During both runs of Data Set 2, participants engaged in eyes open without fixating.

Data Preprocessing

Procedures previously optimized for fcMRI analysis were employed (Fox et al. 2005; Vincent et al. 2006, Van Dijk et al. 2008) based on the method of Biswal et al. (1995). Preprocessing included 1) removing the first 4 volumes to allow for T1-equilibration effects, 2) compensation of systematic, slice-dependent time shifts, and 3) motion correction. Functional data were spatially normalized to the Montreal Neurological Institute (MNI) atlas space using a T2-weighted EPI BOLD-contrast atlas (SPM2, Wellcome Department of Cognitive Neurology, London, United Kingdom) yielding a time series resampled to 2-mm cubic voxels. A low-pass temporal filter removed constant offsets and linear trends over each run while retaining frequencies below 0.08 Hz. A 6-mm full-width half-maximum Gaussian blur was used to spatially smooth the images. Sources of spurious variance, along with their temporal derivatives, were removed through linear regression including 1) 6 parameters obtained by correction for rigid body head motion, 2) the signal averaged over the whole brain, 3) the signal averaged over the lateral ventricles, and 4) the signal averaged over a region centered in deep cerebral white matter. This regression procedure minimized signal contributions of nonneuronal origin including respiration-induced signal fluctuations (Wise et al. 2004; Birn et al. 2006).

Mapping Fronto-Cerebellar Circuitry Using Functional Connectivity

To identify regions that are intrinsically correlated with distinct frontal regions, 2 sites of interest were selected: motor cortex (MOT) and dorsolateral prefrontal cortex (DLPFC). To identify whether the circuits exhibited crossed laterality, separate right and left frontal regions were constructed for each site. Specifically, 8-mm radius spherical seed regions were constructed separately for the right and left hemispheres (i.e., mirrored about the x-axis for each site; MOT coordinates: ±42, –24, 60; DLPFC coordinates: ±42, 16, 36; coordinates reflect the centers of the regions, see Table 1). The particular regions were selected by visual inspection of the anatomical template (for instance, the MOT coordinates were selected so that they fell within the precentral gyrus). Correlation maps were computed for all 4 seed regions for each participant in Data Set 1, and a group-averaged, Fisher's r-to-z transformed correlation map was generated for each seed. These were whole-brain maps; however, here we focus only on the connectivity patterns in the cerebellum. In order to test for crossed laterality, direct comparisons of the left and right MOT and DLPFC seed regions were computed by means of arithmetic subtraction of the z score correlation maps. In this manner, connectivity patterns were generated for each of the separate frontal sites that could reveal the lateralization of the cerebellar connectivity.

Random effects analyses were then conducted to test for statistical significance. Specifically, paired t-tests on the generated $z(r)$ maps were conducted for the left and right seeds of MOT and DLPFC. Only significant results were interpreted. We display the correlation maps (after r-to-z transform) and map differences because they represent the best estimates of the topography. Hypothesis-testing statistics slightly distort the maps due to differential variance across the image (e.g., the center of mass of an object tends to shift away from brain edges in t-maps because of increased variance). For completeness, we also display the full maps based on random effects analysis in the Supplemental Materials.

We next investigated whether the connectivity between a given frontal site and a cerebellar region is reciprocal and selective, that is,

Table 1
Locations of frontal seed regions

Frontal seed		*x*	*y*	*z*
MOT	L	−42	−24	60
	R	42	−24	60
DLPFC	L	−42	16	36
	R	42	16	36
MPFC	L	−12	48	20
	R	12	48	20
APFC	L	−32	40	28
	R	32	40	28

Note: Atlas coordinates (*x*,*y*,*z*) represent the MNI coordinate system (Evans et al. 1993) based on the MNI152/ACBM-152 target.

Table 2
Locations of cerebellar correlation peaks with frontal cortex

Frontal seed	Label	Peak cerebellar coordinate			*z*(*r*)
L MOT	Lobule V	**22,**	**−52,**	**−22**	0.26
	Lobule VIIIB	20,	−58,	−54	0.23
R MOT	Lobule V	**−20,**	**−50,**	**−24**	0.28
	Lobule VIIIB	−19,	−57,	−53	0.21
L DLPFC	Crus I	**10,**	**−82,**	**−26**	0.35
	Crus II	36,	−68,	−44	0.32
	Crus I	−36,	−66,	−40	0.17
R DLPFC	Crus I	**−12,**	**−82,**	**−28**	0.36
	VIIB	−36,	−70,	−46	0.32
	Crus I	12,	−82,	−28	0.19
L MPFC	Crus I	**34,**	**−80,**	**−36**	0.29
	Crus I	−30,	−78,	−34	0.26
R MPFC	Crus I	**−32,**	**−76,**	**−34**	0.29
	Crus I	24,	−80,	−32	0.20
L APFC	Lobule VI/Crus I	**36,**	**−52,**	**−34**	0.21
	Lobule VI	−36,	−52,	−34	0.22
R APFC	Lobule VI	**−36,**	**−52,**	**−34**	0.29
	Lobule VIIB/Crus II	38	−46,	−48	0.23

Note: Atlas coordinates and abbreviations for cortical regions are similar to Table 1. R = right, L = left. Coordinates in bold correspond to the centers of seed regions that were drawn in cerebellar cortex in order to compute correlation maps for the cerebral cortex (see Figs. 2 and 7). Labels represent approximate lobule locations based on the MRI atlas of the human cerebellum (Schmahmann et al. 1999, 2000)

whether maps produced by cerebellar seed regions exhibit "closed-loop circuitry" by showing preferential correlations with those frontal sites that originally produced the cerebellar correlations. Note that this is not an obligatory property. It is possible that cerebellar seeds could correlate with widespread regions of the cerebral cortex or that all would preferentially correlate with MOT. To test for closed-loop circuitry, we identified the peaks of functional connectivity in the cerebellum in the MOT map (CBM_{MOT}) and in the DLPFC map (CBM_{DLPFC}). Spherical regions of 2-mm radius were defined around these cerebellar peaks (CBM_{MOT} coordinates, Right: 22, −52, −22; Left: −20, −50, −24; CBM_{DLPFC} coordinates, Right: 10, −82, −26; Left: −12, −82, −28; see Table 2) and the corresponding correlation maps were computed for the cortex. The circuit properties were then tested by exploring to what degree the cerebellar regions projected to separate or overlapping regions of the cerebral cortex. Specifically, we predicted that the CBM_{MOT} seed would result in selective correlations with MOT and would not correlate with prefrontal regions, and that the CBM_{DLPFC}-correlated regions would correlate with prefrontal cortex and would spare the motor strip.

It is important to emphasize again that fcMRI does not permit recovery of information about the "directionality" of connections (Allen et al. 2005). That is, seeding a region in the cerebellum will likely result in correlations with both the efferent and the afferent connections to it; functional connectivity analysis only assesses the degree of correlation between spontaneous activity in different regions, not the direction of influence. Nonetheless, fcMRI remains a valuable method for investigating the topography of connectivity between brain regions, especially when the circuits under consideration exhibit separable correlation profiles.

Cerebellar Topography

As the results of the preceding analyses will show, functional connectivity reveals distinct fronto-cerebellar circuits when comparing a dorsolateral prefrontal region with a motor region. Based on this result, we next extended the approach to explore fronto-cerebellar topography more extensively. Tracing studies in the monkey suggest that there are multiple prefrontal zones that project to the pontine nucleus, as well as other zones that markedly lack pontine projections (Schmahmann and Pandya 1997; Middleton and Strick 2001). Importantly, previous diffusion imaging work has presented initial evidence that human prefrontal cortex may contribute relatively more projections to the pontine nucleus than does monkey prefrontal cortex (Ramnani et al. 2006), but the topography of fronto-cerebellar connectivity has not yet been characterized.

Two additional frontal regions (for a total of 4) were targeted: medial prefrontal cortex (MPFC) and anterior prefrontal cortex (APFC), and again bilateral 8-mm radius, spherical regions were drawn (MPFC: ±12, 48, 20; APFC: ±32, 40, 28) (Table 1). The corresponding correlational maps were computed for each participant and a *z* transformed, group-averaged map was generated. The subtraction method was again employed to assess the differential correlation patterns found in the cerebellum from each of the MOT, DLPFC, MPFC, and APFC seed regions. Random effects analyses formally quantified the statistical significance of the correlation maps for selective pairs of the seed regions. Effects were interpreted only if they were significant (corresponding to $P < 0.05$ correcting for multiple comparisons using the False Discovery Rate method).

Anticipating the results, multiple regions of correlated activity were found in the cerebellum for each frontal site. Using the same approach that was applied to the MOT and DLPFC maps above, peak search was employed on the MPFC and APFC maps to obtain local maxima in the cerebellum (CBM_{MPFC} coordinates: 34, −80, −36 and −32, −76, −34; CBM_{APFC} coordinates: ±36, −52, −34) (Table 2). Spherical 2-mm radius seed regions were created around them to compute correlation maps for the cerebral cortex. The previous analysis compared cortical networks resulting from seeding anterior and posterior cerebellar regions. This test enabled us to assess the extent to which different locations in the posterior cerebellum are functionally coupled with the similar or distinct cortical networks.

Control Analyses

An important internal control for our investigation is to show that seeding regions in the cerebral cortex known to lack anatomic connections with the cerebellum will similarly fail to produce fcMRI correlations in the cerebellum. Research in the rhesus monkey suggests that striate cortex does not have any projections to the pons—an obligatory step to the cerebellar cortex—although other regions in the occipital cortex do (Schmahmann and Pandya 1993). Accordingly, we placed bilateral 8-mm radius seeds in or near primary auditory and visual cortices (AUD: ±46, −18, 8; VIS: ±4, −88, 2).

As an additional control, we investigated the sensitivity of the overall pattern of cerebellar topography to our choice of particular seed locations in frontal cortex. Accordingly, we created new pairs of frontal seeds several millimeters away from the coordinates of the original seeds, taking care that the seed remained in the same general frontal zone (for instance, the new MOT seeds were moved approximately 8 mm medially, while remaining in the precentral gyrus). Because we were interested in the overall cerebellar topography resulting from each region, the correlation maps from

the left and right seed regions were averaged together to increase statistical power.

Replication and Dissociation of Fronto-Cerebellar Circuits

As the results will reveal, multiple distinct fronto-cerebellar circuits are observed. To formally test whether these circuits can be dissociated, we extracted their corresponding seed regions in the cerebellum and frontal cortex and formally tested, in an independent data set, whether differential correlation could be replicated. For this analysis, we asked whether each circuit demonstrated preferential correlation that was greater between its cerebellar seed and frontal target than any of the other frontal targets. Specifically, the cerebellar topography generated by the different frontal seed regions (MOT, DLPFC, MPFC, and APFC) in Data Set 1 was used to define cerebellar regions that were used as a priori seeds in Data Set 2 (Vincent et al. 2006, 2008; Kahn et al. 2008). Bilateral 2-mm radius spherical seeds were constructed around local maxima in the cerebellum maps generated from each bilateral frontal seed pair in Data Set 1. These regions were then used as seeds in Data Set 2 to test the prediction that 4 distinct fronto-cerebellar circuits exist. Two-way *t*-tests directly compared correlation strengths between each site in the cerebellum and each frontal region of interest, yielding 12 comparisons in total.

Results

Seed-based fcMRI was used to map fronto-cerebellar circuits in the human. We first provide evidence that the governing principles of these same pathways in nonhuman primates, for instance, the crossed laterality of the cerebro-cerebellar connections, are present in humans and can be detected using fcMRI. We next show that the human cerebellum contains at least 4 distinct fronto-cerebellar circuits, including 3 associated with distinct prefrontal regions. Importantly, control seeds placed in or near primary auditory and visual cortices do not produce correlations in the cerebellar hemispheres. In a final analysis, we directly demonstrate that the 4 dissociated fronto-cerebellar circuits replicate in an independent data sample.

Figures show connectivity maps overlayed onto an anatomical template generated by averaging the T1 structural scans of all of the participants in the present study. To assist visualization, the volumetric results are also projected onto the inflated cortical surface of the PALS (population-average landmark- and surface based) atlases of the cerebrum (Fig. 2) and of the cerebellum (Fig. 8) using Caret software (Van Essen 2005). Anatomic description of the cerebellum is based on Schmahmann et al. (2000).

fcMRI Reveals Contralateral Lateralization of Fronto-Cerebellar Connectivity

Cerebellar connectivity generated by subtracting the MOT and DLPFC maps from their contralateral counterparts is shown in Figure 1. Anatomically selective regions of the cerebellum reveal robust correlations with the 2 sets of frontal seeds. Cerebellar connectivity shows crossed lateralization in relation to the cortex.

From a technical perspective, these results provide further evidence that spontaneous BOLD fluctuations are constrained by anatomical projections (Biswal et al. 1995; Fox and Raichle 2007; Vincent et al. 2007; Johnston et al. 2008). It is especially compelling in the present case as the contralateral connectivity pattern observed cannot be attributed to artifacts such as shared vasculature—the cerebellum is supplied by its own major arteries (Schmahmann 2007b)—or to head motion. Moreover, there are no direct anatomic projections between the cerebral cortex and cerebellum. Thus, the results reinforce that fcMRI correlations can reflect polysynaptic connectivity.

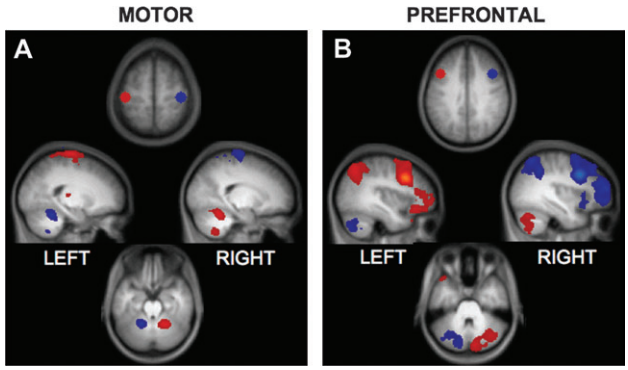

Figure 1. Motor and prefrontal cortex project to distinct, preferentially contralateral regions of the cerebellum. Correlation maps for motor and prefrontal seed regions are displayed overlaid on the participants' averaged T1 structural scan. (*A*) Bilateral spherical seed regions in MOT (MOT coordinates: ±42, −24, 60) correlate with regions in lobules IV–VI in the anterior cerebellum and with VIIIB in ventral aspects. (*B*) Bilateral seed regions in DLPFC (DLPFC coordinates: ±42, 16, 36) correlate with distinct regions in Crus I and Crus II in the posterior cerebellum. In each map, red corresponds to preferentially greater correlations with seed regions in the left hemisphere and blue corresponds to preferentially greater correlations with seed regions in the right hemisphere. Maps are at a threshold of $z(r) > 0.1$. All image sections and atlas coordinates are referenced to the MNI coordinate system (Evans et al. 1993). Left is displayed on the left.

Motor and Prefrontal Cortex Form Independent Circuits with the Cerebellum

Cerebellar correlations with MOT versus DLPFC seed regions reveal clear anatomic dissociation (Fig. 1). MOT correlations recover the dual motor representations in the anterior–superior cerebellum and in the inferior cerebellum (Fig. 1*A*), consistent with the expected topography of primary and secondary representations (Snider and Eldred 1951; Grodd et al. 2001), whereas DLPFC correlations are found in the posterior hemispheres (Crus I/II, Fig. 1*B*). The cerebellar regions associated with MOT correspond to lobules IV–VI and VIIIB (lobule locations estimated based on Schmahmann et al. 1999, 2000). Importantly, these lobules contain a preponderance of labeled neurons from viral injections to M1 in the cebus monkey (Kelly and Strick 2003). The DLPFC correlations (Fig. 1*B*) appear in regions that correspond to Crus I and Crus II of the cerebellum (Schmahmann et al. 1999, 2000), which contain the majority of labeled neurons from viral injections in monkey prefrontal area 46 (Kelly and Strick 2003). Random effects analyses comparing left and right MOT and DLPFC maps are displayed in Supplementary Figure 1.

Further analysis revealed that seeding the peaks of the cerebellar regions recovered from the preceding analysis results in correlations with distinct cerebral networks. Figure 2*A* displays the 2 networks that are correlated with cerebellar seeds CBM_{MOT} and CBM_{DLPFC} (locations of seeds displayed in Fig. 2*B* and listed in Table 2), projected onto the inflated cortical surface (peak frontal coordinates and $z(r)$ values listed in Supplementary Table 1). Importantly, cortical regions correlated with these 2 cerebellar sites were nonoverlapping, supporting the characterization of certain cerebral–cerebellar circuits as closed, segregated loops (Kelly and Strick 2003).

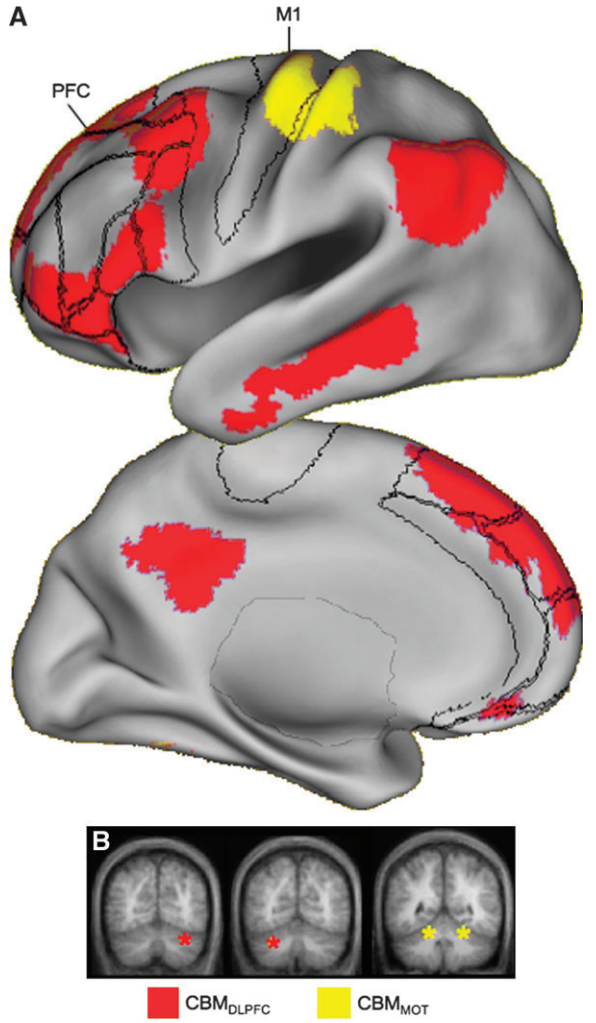

Figure 2. Projections from the cerebellum form closed-loop circuits. Regions in the anterior and posterior cerebellar hemispheres correlate with distinct, nonoverlapping cerebral networks. (*A*) Regions correlated with CBM_{MOT} (lobule V) are restricted to the MOT in the frontal lobe, whereas regions correlated with CBM_{DLPFC} (Crus I) include lateral dorsal, ventral as well as medial PFC. Note that the CBM_{MOT}-correlated region at the base of the temporal lobe on the medial view is most likely actually correlated activation in the cerebellum that has "spilled over" into the cerebral cortex because of the cortical inflation and does not actually reflect correlations in the temporal lobe. Maps are at a threshold of $z(r) > 0.1$. The volumes are projected onto the left hemisphere cortical surface of the PALS atlas (Van Essen 2005). The right hemisphere produces indistinguishable results. Borders reflect approximate borders of relevant Brodmann areas encompassing the prefrontal cortex and MOT (see Fig. 7). M1 = Primary motor cortex, PFC = Prefrontal cortex. (*B*) Locations of the seed regions are shown schematically (colored asterisks) on slices of the cerebellum.

The Cerebellum Contains (at least) 4 Distinct Projection Zones from the Frontal Cortex

Having established that fcMRI can map distinct fronto-cerebellar circuits, we next extended the approach to map the cerebellar targets of 4 separate frontal regions: MOT, DLPFC, MPFC, and APFC. For these analyses, because between-circuit contrasts were the target and not evidence for lateralization, bilateral seeds were used to increase statistical power. Figure 3 displays subtractions between 2 given maps, effectively revealing the relative differences in correlation patterns for different fronto-cerebellar connections.

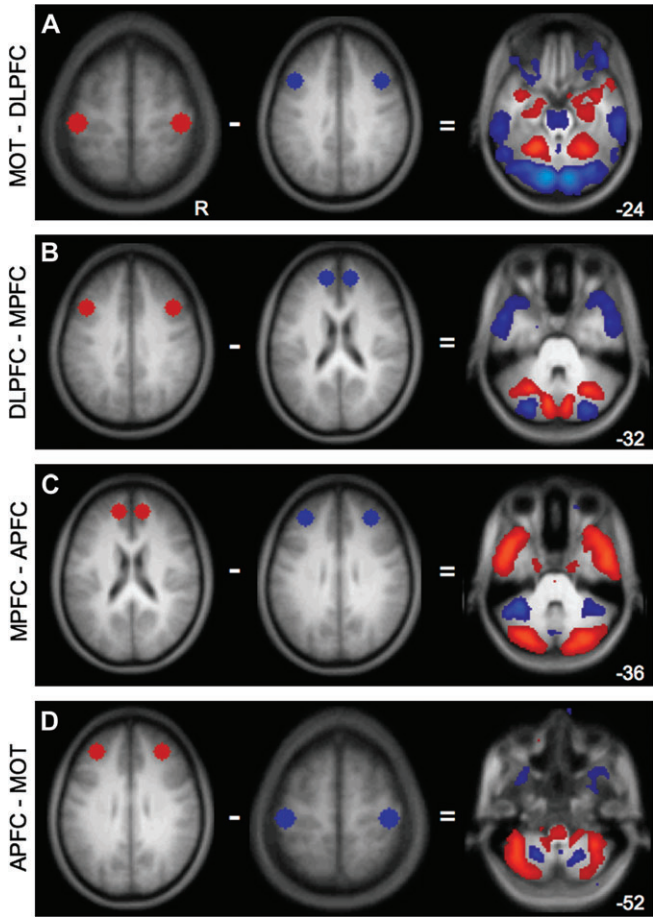

Figure 3. The cerebellum contains at least 4 distinct zones associated with frontal cortex. To illustrate the presence of multiple fronto-cerebellar circuits, maps from distinct frontal seeds are directly compared. Each panel shows the regions being subtracted (left) and the resulting correlation map (right). Maps are at a threshold of $z(r) > 0.1$. (*A*) MOT–DLPFC results in preferential correlations with MOT in lobule V in the anterior hemisphere as well as in lobule VIIIB. Preferentially DLPFC-correlated regions include Crus I, Crus II, VIIB, and IX. (*B*) DLPFC–MPFC further divides the posterior cerebellum: MPFC has greater correlations with Crus I, whereas DLPFC has relatively greater correlations with Crus II (*C*) MPFC–APFC dissociates in anterior cerebellum betweeen Crus I and lobule VI, respectively. In ventral cerebellum, MPFC preferentially correlates with IX, whereas APFC correlates with VIIIA. (*D*) APFC–MOT: APFC preferentially correlates with VI, whereas MOT correlates with lobule V in the anterior lobe. APFC continues to correlate with the extent of VI moving ventrally and also appears to correlate with VIIB–VIIIA and Crus II at the ansoparamedian fissure, whereas MOT retains correlations in VIIIB. Numbers refer to the *z* coordinate plane of the cerebellar slice.

All comparisons show dissociations in the topography of the cerebellar correlations based on connectivity with the different frontal regions. Figure 3*A* exhibits the dissociation of cerebellar connectivity with MOT and DLPFC seeds, respectively, as discussed above. Figure 3*B* shows further fractionation of posterior cerebellum by comparing DLPFC with MPFC. Specifically, MPFC-correlated regions of the cerebellum localize to lobule Crus I, whereas DLPFC-correlated regions span Crus I as well as Crus II in its lateral and ventral extent (Schmahmann et al. 1999, 2000). APFC correlations, relative to MPFC correlations, appear largely in lobule VI (Fig. 3*C*) and more ventrally in VIIIA. MOT and APFC correlations dissociate between lobules VIIIB and VIIIA/VIIB in ventral cerebellum (Fig. 3*D*) and between lobules V and VI in dorsal cerebellum (data not shown). The results from the random effects analyses

Table 3
Peak cerebellar coordinates from frontal seeds

Contrast	Label		Coordinate			*z*(*r*)
MOT–DLPFC	L	Lobule VIIIB	−24	−54	−56	0.33
	L	Lobule V	−20	−52	−22	0.32
	R	Lobule VIIIB	20	−60	−56	0.28
	R	Lobule V	24	−54	−20	0.27
DLPFC–MPFC	L	VIIB	−34	−68	−50	0.32
	L	Crus II	−10	−76	−28	0.31
	R	Crus II	10	−78	−25	0.28
	R	Crus II	34	−70	−50	0.25
MPFC–APF	R	IX	6	−54	−48	0.41
	R	Crus I	26	−82	−34	0.39
	L	Crus I	−26	−82	−34	0.38
APFC–MOT	L	VI/Crus I border	−34	−54	−34	0.43
	L	VI	−30	−66	−28	0.41
	R	VI/Crus I border	36	−56	−32	0.32
	L	VIIB/VIIA border	−38	−46	−46	0.31
	L	VI	−34	−66	−26	0.31
	L	Crus I	−46	−54	−36	0.29
	R	VIIB/VIIA border	38	−48	−48	0.26

Note: Atlas coordinates and abbreviations for cortical regions are similar to Table 1. R = right, L = left. Labels represent approximate lobule locations based on the MRI atlas of the human cerebellum (Schmahmann et al. 1999, 2000).

comparing cerebellar connections with different frontal sites are shown in Supplementary Figure 2 (peak coordinates and *t*-scores summarized in Table 3).

We are cautious about claiming precise anatomical localization of our findings due to the smoothing and averaging of our functional data. However, in addition to the group-averaged maps, we also inspected the maps of individual subjects to determine whether the same general patterns also hold at the single-subject level. Figure 4 shows the results of the above comparisons carried out in 3 subjects projected onto their respective anatomical volumes. The dissociations in the cerebellum are evident even at the individual-subject level.

The specificity of the cerebellar effect is particularly prominent when the background correlations that are common between the left and right seeded maps are removed via the subtraction method. As shown in Figure 5, raw correlation maps of the cerebellum without subtraction reveal bilateral functional connectivity (peak correlation coordinates in Table 2); the contralateral cerebellum shows relatively stronger connectivity that becomes prominent when the right and left hemisphere seeded maps are directly contrasted (as in Fig. 1). These observations are consistent with the known contralateral, polysynaptic connections between cerebral cortex and the cerebellum (Schmahmann 1996; Middleton and Strick 2001; Kelly and Strick 2003). It should also be noted that in all of our analyses, we saw robust connectivity with the thalamus, which is the obligatory anatomical step in projections from the cerebellum to the cerebral cortex (see also Zhang et al. 2008). We could also detect correlations in the pons but not in all instances (Fig. 3).

Cerebro-Cerebellar Circuits Are Not Detected for Primary Auditory and Visual Cortices

All of the frontal sites tested resulted in robust functional correlation with different parts of the cerebellum. However, in order to interpret these differences it is equally important to demonstrate that cerebellar correlations are also selective. To this end, we seeded regions in or near primary auditory (Heschl's gyrus) and primary visual cortex, both of which do not appear to project to the cerebellar hemispheres (Huffman and Henson 1990; Schmahmann and Pandya 1993). The results of these analyses are displayed in Figure 6, which also includes correlation maps produced from MOT and DLPFC for comparison purposes. In keeping with expectations, although the auditory and visual seeds produced robust cortical correlations, they failed to correlate with activity in the cerebellar hemispheres.

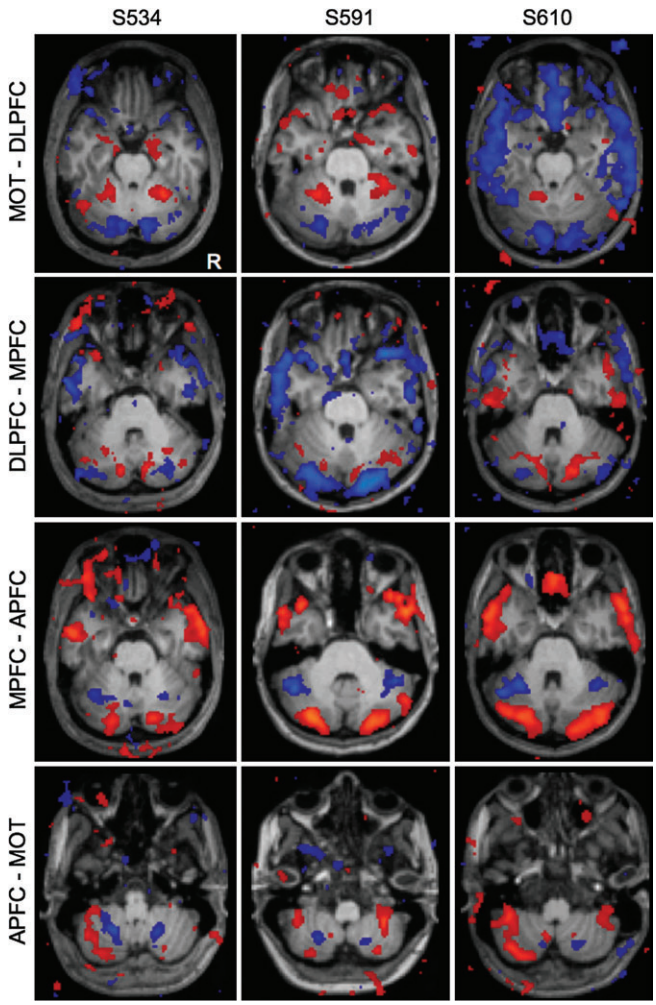

Figure 4. Fronto-cerebellar circuits in individual subjects. The same comparisons in Figure 3 are computed individually for 3 representative subjects. Results are overlayed on each subject's own anatomical volume. Although the locations of the peak correlations vary somewhat, the overall pattern of functional connectivity is similar to that seen at the group level.

A Map of Cortical Projection Zones from the Cerebellum

Our final inquiry assessed the distribution of cortical connectivity resulting from seeding the dissociated regions in the cerebellum that were each linked to distinct prefrontal regions. We have already demonstrated that regions in lobule V and Crus I of the cerebellum are correlated with nonoverlapping cerebral networks (Fig. 2). Figure 7 displays the result of seeding different regions within the posterior lobe of the cerebellum (cerebellar seed coordinates in Table 2). These particular regions were chosen to be seeds because they were found to be the most strongly correlated with the 3

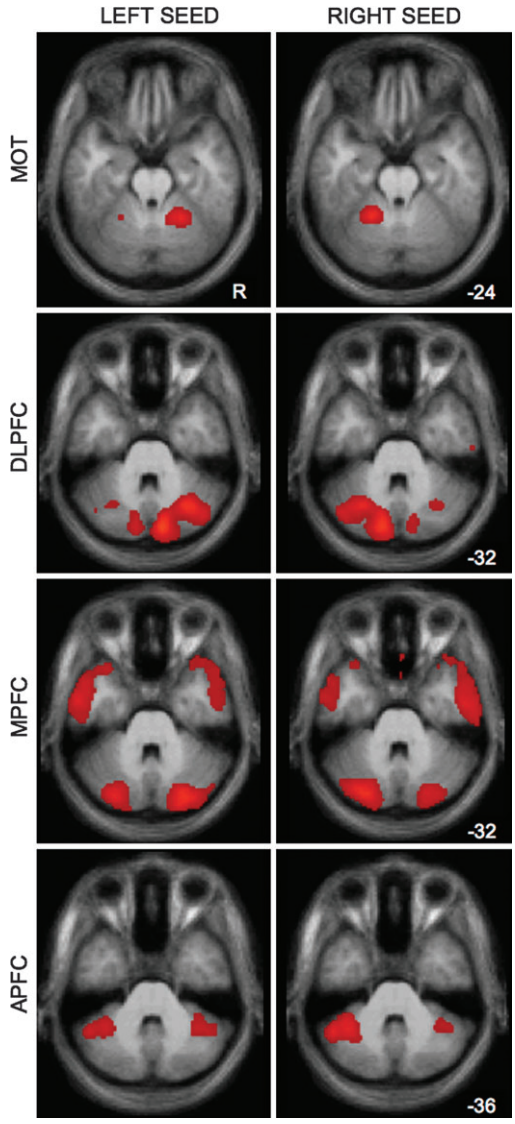

Figure 5. Raw correlation maps show some bilateral cerebellar connectivity from unilateral cortical seeds. Although subtraction of left and right seeds in a given cortical region highlights the contralateral organization of cerebellar connectivity (see Fig. 1), the raw left and right seeds show present, but weaker, ipsilateral connectivity with the cerebellum. This observation is consistent with the smaller percentage of cerebellar projections that cross back to the ipsilateral hemisphere (see text). Maps are at a threshold of $z(r) > 0.1$.

frontal sites. Seeding other peak foci in the cerebellar maps, for instance the secondary foci in lobule VIII from the MOT seed, would presumably produce comparable results. Although largely different cortical networks are obtained, there is also a good deal of overlap in the networks for the 2 most posterior seeds (located in Crus I and the Crus I/Crus II border of the cerebellum, see Fig. 7*B*). This can also be appreciated in Table 2 and Figure 8, which illustrate that both DLPFC and MPFC seeds produce strong correlation peaks in Crus I. Thus, cerebellar regions associated with prefrontal cortex are embedded within distinct cortical circuits but these circuits are not entirely independent at the resolution explored here.

A Map of Cerebellar Topography

As a summary of our findings, a comprehensive map of the cerebellar correlations with the 4 frontal regions is shown in slice view as well as projected onto the cortical surface of the cerebellum in Figure 8. Although some overlap of correlated regions does occur—between DLPFC and MPFC and between DLPFC and APFC—the segregated topography of cerebellum is nonetheless impressive. Each of the 4 frontal regions correlates with distinct cerebellar regions.

The results of displacing each seed while remaining within the 4 frontal zones is displayed in Supplementary Figure 3. Note that despite moving the seeds at least 8 mm from the original locations, the cerebellar topography remains remarkably similar to that shown in Figure 5. This implies that the overall topography of fronto-cerebellar connectivity we show here is not merely a product of the idiosyncratic choice of coordinates within the 4 frontal zones we investigated. On the other hand, it also implies that the resolution applied here may not be able to investigate fine-grained differences in connectivity with the cerebellum.

The presence of segregated circuits that involve 3 distinct prefrontal regions confirms that the cerebellum participates in multiple different networks subserving cognition. Relevant to recent interest in the "default network," which includes MPFC (Gusnard et al. 2001; Buckner et al. 2008), the cerebellar region correlated with MPFC (Fig. 8) is a prominent component of the default network. In fact, seeding this region results in correlations in the cerebral cortex that nearly fully encompass the cortical regions that comprise the default network (Fig. 7). Taken as a group, the regions of the cerebellum linked to prefrontal cortex occupy a significant portion of the posterior hemisphere suggesting that, in humans, a large portion of the cerebellum may be dedicated to supporting cognitive functions.

Fronto-Cerebellar Circuits Replicate and Dissociate in an Independent Data Sample

The analyses above map 4 distinct fronto-cerebellar circuits. To formally explore whether the circuits dissociate, we extracted seed regions in frontal cortex and the cerebellum from Data Set 1 and tested them for segregation in the independent Data Set 2. Specifically, we predicted a quadruple dissociation between cerebellar regions that preferentially correlate with 4 different zones in the frontal cortex. This is a stringent and conservative prediction: The correlation between each cerebellar region and its prefrontal target was predicted to be significantly stronger than any of the other 3 prefrontal targets. Results confirmed this prediction for each of the 4 cerebellar regions (Fig. 9): Two-tailed *t*-tests between each frontal region and each cerebellar zone revealed that correlations between lobule V and MOT, between Crus I and DLPFC, between Crus II and MPFC, and between lobule VIIIA and APFC were significantly stronger than any other pairing of these cerebellar and frontal sites (all $P < 0.001$). These results demonstrate that the cerebellar regions under consideration reliably and preferentially correlate with different frontal regions within the cerebellum.

Discussion

Leiner et al. (1986) proposed that the cerebellum exerts influence over nonmotor functions. Viral and conventional tracing techniques in nonhuman primates (Middleton and Strick 1994, 2001; Schmahmann and Pandya 1997; Dum and Strick 2003; Kelly and Strick 2003) and neuroimaging and neuropsychological techniques in humans (Petersen et al. 1989; Fiez et al. 1992; Desmond and Fiez 1998; Schmahmann

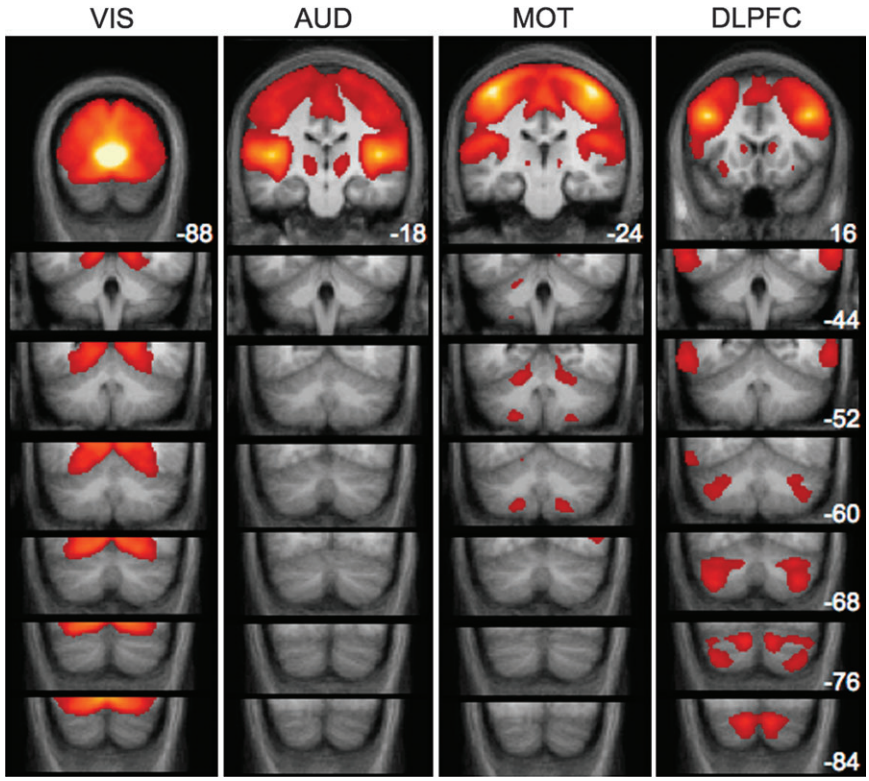

Figure 6. Cerebellar regions are not correlated with primary visual and auditory cortices. Although seeding striate cortex (VIS) and Heschl's gyrus (AUD) produces robust correlations in the cerebral cortex, no connectivity appears to be present in the cerebellum. Correlations with each of the 4 cerebral regions are displayed in successive coronal slices of the cerebellum. Maps are thresholded at $z(r) > 0.1$. MOT and DLPFC correlations are shown for comparison purposes. The location of the seed regions corresponds to the highest intensity values (white/yellow patches) in the first panel of each column. Numbers correspond to the *y* coordinate of each coronal slice.

2004; Ravizza et al. 2006; Schmahmann 2007a; O'Reilly et al. 2008; Schmahmann and Pandya 2008) all point compellingly to a role for the cerebellum in cognition. However, little is known about the topography of the human cerebellum in relation to fronto-cerebellar circuits. Here, we map human cerebellar topography using functional connectivity and demonstrate the presence of 4 separate fronto-cerebellar circuits including 3 distinct circuits that associate with prefrontal cortex (Fig. 7).

As a group, the regions of the cerebellum functionally coupled with prefrontal cortex occupy a significant extent of the posterior hemisphere. Interestingly, the prefrontal-coupled regions of cerebellum in particular appear to have undergone significant expansion in recent hominid evolution. We also note that the network of cortical regions correlated with a particular lobule in posterior cerebellum, Crus I, is similar to the default network (Raichle et al. 2001; Buckner et al. 2008). Thus, the human cerebellum contains multiple regions that are correlated with distinct areas of prefrontal cortex. Functional understanding of the cerebellum should consider these distinctions.

Early anatomical work demonstrated that the dentate nucleus projects to regions of the thalamus with known connections to association areas of cerebral cortex (for a review see Leiner et al. 1986), providing an initial hint of the neural architecture that could support cerebellar influence on these areas. However, the application of both antereograde and retrograde viral tracers in the monkey provided the most compelling evidence for this hypothesis by showing that different areas of cortex that include prefrontal areas participate in closed circuits with different regions of the cerebellum (Middleton and Strick 2000, 2001; Kelly and Strick 2003). Our use of fcMRI produces results consistent with the known anatomy of cerebro-cerebellar connections.

On the basis of the tracing work, we expected to find crossed laterality in our fronto-cerebellar correlation maps. Though all cortical regions were preferentially correlated with contralateral cerebellum as predicted (i.e., MOT and DLPFC), bilateral connectivity was present for all regions tested to varying degrees (i.e., Fig. 5). Although connectional architecture is mostly crossed, a moderate number of projections from neocortex (20–30%) terminate—via the pons—on ipsilateral cerebellum. Similarly, the pathway from cerebellum to the thalamus is predominantly, but not wholly, crossed (Schmahmann 1996).

Inspection of the raw correlation maps (Fig. 5) suggests that the MOT seeds produce relatively few ipsilateral correlations compared with the more robust bilateral pattern seen for the 3 prefrontal seed regions. Future work on this topic can determine whether this is a meaningful functional or anatomic difference. It is also possible that the ipsilateral cerebellar correlations reflect correlations with the "frontal" site contralateral to the original neocortical seed. A neocortical seed in one hemisphere often produces robust correlations with the same region in the opposite hemisphere (Biswal et al. 1995), presumably reflecting strong interconnectivity of these regions via the corpus callosum (Johnston et al. 2008). Therefore, ipsilateral cerebellar correlations could arise indirectly via the correlated contralateral neocortex.

As predicted, we observed intrinsic, correlated activity between MOT and the anterior cerebellar hemispheres and

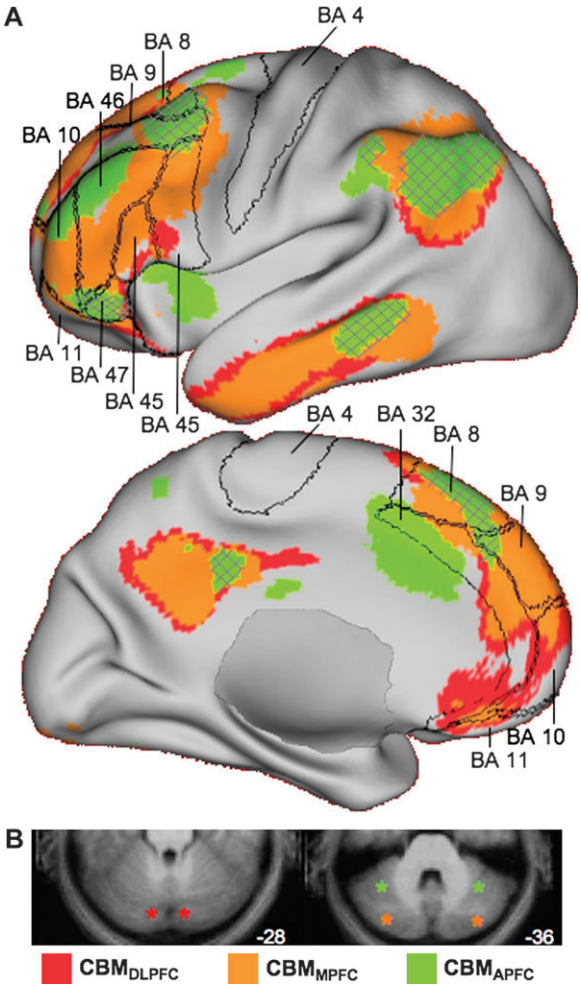

Figure 7. Neighboring regions of the cerebellum participate in distinct, yet partially overlapping, cerebral networks. (*A*) Cortical connectivity with bilateral CBM_{DLPFC}, CBM_{MPFC}, and CBM_{APFC} seeds did not show the same strict segregation that was seen in the comparison between CBM_{DLPFC} and CBM_{MOT} (Fig. 2). These regions, especially CBM_{DLPFC} and CBM_{MPFC}, appear to participate in distributed cortical networks that converge in dorso-, ventro-, and medial PFC, at the posterior midline, and in regions of the lateral parietal and temporal lobes. The CBM_{APFC} network appears to be segregated from the other 2 networks in the prefrontal cortex, though some convergence was also seen, for example, in BA 47. Borders reflect approximate borders of relevant Brodmann areas encompassing the prefrontal cortex and motor cortex. Hatched regions represent overlap of the CBM_{APFC} correlation map with the 2 other networks. BA = Brodmann area. (*B*) Schematic representation of the seed locations (asterisks) on cerebellar slices. CBM_{DLPFC} coordinates: ±12, −82, −28; CBM_{MPFC} coordinates: 34, −80, −36 and −32, −76, −34; and CBM_{APFC} coordinates: ±36, −52, −34.

lobule VIIIB and between DLPFC and the posterior cerebellar hemispheres. Examining our results in more detail reveals a fractionation of the posterior cerebellum into regions that preferentially correlated with MPFC relative to DLPFC (such as Crus I) and vice versa (Crus II). Additionally, we found that placing a seed region in APFC resulted in correlated activity in dorsal lobule VI and ventral VIIB–VIIIA, defining a fourth zone (which can also be distinguished from MOT representations). The cerebellar topography resulting from motor and DLPFC seeds is consistent with established anatomical connectivity in the monkey.

We additionally provide strong evidence that there are at least 2 other circuits connecting the cerebellum to medial and anterior prefrontal cortices in humans. Studies in nonhuman primates suggest that there are some projections to the pons from dorsomedial prefrontal convexities but not from ventrolateral or orbitofrontal cortices (for a summary see Schmahmann and Pandya 1997). Our map of cortical correlations with the posterior cerebellar hemispheres (Fig. 7) suggests the possibility that there exist cerebro-cerebellar circuits in human prefrontal cortex that may not find a homologue in monkeys. Placing seeds in primary auditory and visual cortices did not produce correlations in the cerebellum, providing an internal control for our results.

The observation that extensive portions of the posterior cerebellum are associated with putatively "cognitive" networks is especially interesting in light of the suggestion that phylogenetic expansion of certain lateral and posterior aspects of the cerebellum and cerebellar nuclei has paralleled the expansion of the frontal cortex (Rilling and Insel 1998; MacLeod et al. 2003; Whiting and Barton 2003). The ventral half of the dentate nucleus, which comprises the fiber connections to prefrontal cortex, is more developed in humans than in great apes (Middleton and Strick 1994, 2001; Matano and Hirasaki 1997; Matano 2001; Dum and Strick 2003; Akkal et al. 2007). Further, relative to cerebellar midline (vermis), the lateral hemispheres of the cerebellum have undergone significant expansion in hominoids relative to monkeys (MacLeod et al. 2003). The thalamus and pons, relay stations between the cerebellum and the neocortex, have also displayed correlated evolutionary development (Whiting and Barton 2003). The preferential expansion of these particular cerebellar regions may contribute to cognitive functions particularly well developed in humans, such as language and reasoning (Leiner et al. 1991, 1993).

Interestingly, seeding a region in Crus I resulted in a pattern of correlated cortical activity including MPFC that resembles the default network (Fig. 7)—a network of cortical regions linked to social cognition, remembering, and planning the future (Gusnard and Raichle 2001; Svoboda et al. 2006; Buckner and Carroll 2007; Buckner et al. 2008; Spreng et al. 2009).

Caveats

Several caveats and open questions must be considered when interpreting functional connectivity results. A pertinent issue to the present study is to what degree functional connectivity reflects underlying structural connectivity. The observation that DLPFC and MOT seed regions produced correlated regions in the cerebellum that are predicted by the monkey tracing work suggests that fcMRI respects anatomical constraints. Additionally, our control seeds in or near striate and primary auditory cortex did not produce correlations in the cerebellum, consistent with known anatomy. However, fcMRI connectivity is inherently a more pervasive measure than anatomical connectivity because 2 regions can be correlated with one another just by virtue of the fact that they participate in a common functional network.

One implication of the possibility of indirect correlations for the present study is that other regions outside of the frontal cortex may drive the coherence patterns observed between the neocortex and the cerebellum. For example, seeding the posterior cerebellum (Crus I) produced a distributed network of correlations similar to the default network, including MPFC, the inferior parietal lobule and the posterior cingulate (Fig. 7). Although MPFC was identified as the neocortical region exhibiting the strongest correlations with Crus I, we cannot rule

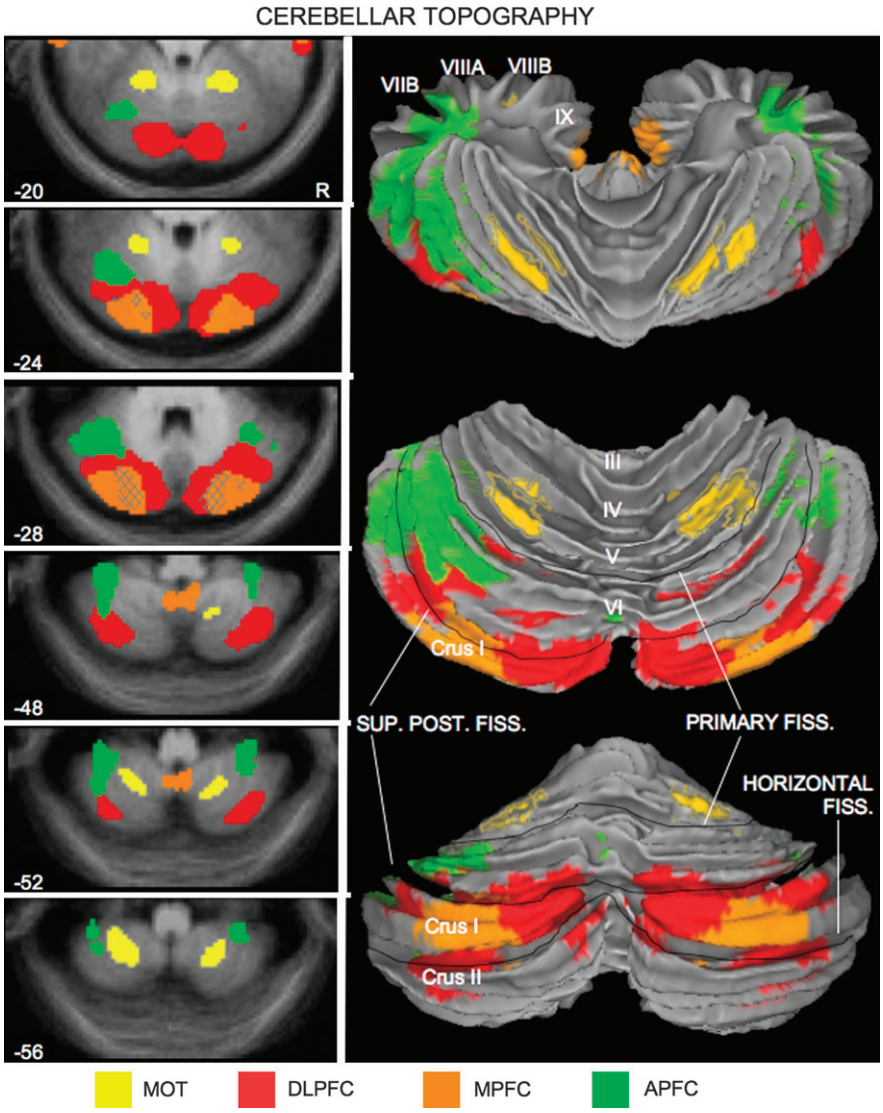

Figure 8. A provisional map of human cerebellar topography. All of the data in the present study were combined to provide an estimate of cerebellar topography based on the 4 dissociated regions illustrated in Figure 3. Correlations with the 4 frontal regions are illustrated for descending transverse sections of the cerebellum in the left panel. Each map is based on the averaged ($N = 40$) $z(r)$ correlation map (threshold = $z(r) > 0.1$). Hatched regions represent overlap of 2 correlation maps. The $z(r)$ correlation maps are projected onto the cortical surface of the cerebellum in the right panel to illustrate the topographical organization of the fronto-cerebellar connectivity. This map provides a provisional (and certainly incomplete) characterization of the human cerebellum based on connectivity to the frontal cortex. The top projection is a superior view looking down on the rostral and dorsal faces of the cerebellum; the bottom projection shows the view from behind. The middle projection is a rotation between the other 2 (showing the entire dorsal face) to emphasize the relationships among all 4 dissociated cerebellar zones. Note that the majority of the mapped portion of the posterior cerebellum is associated with prefrontal (cognitive) regions of the neocortex. Anatomical labels and major divisions based on the MRI atlas of the human cerebellum (Schmahmann et al. 1999, 2000).

out the possibility that another region within that network, for example, the posterior cingulate, could mediate the relationship between MPFC and the cerebellum or contribute to the correlations in the cerebellum. For instance, parietal cortex has known anatomical connections with the cerebellum (Clower et al. 2001). This may also explain why regions in inferior temporal cortex exhibit correlations with regions in the cerebellum (i.e., Fig. 7) despite evidence from tracing work that few, if any, projections exist between the pons and inferior temporal cortex (Glickstein et al. 1985; Schmahmann and Pandya 1991). Similarly, neocortical regions contralateral to a seed region may be responsible for driving the ipsilateral cerebellar response (Fig. 5).

Functional connectivity in other animals for which anatomical pathways are well characterized may help to resolve these questions. However, it is important to note that although the issue of pervasiveness makes the overlap of 2 correlation maps difficult to interpret, it does not undermine the interpretation of correlated networks that are clearly segregated; fcMRI remains a powerful technique for detecting divergent networks and for characterizing the topography of regions participating in them.

Conclusions

Our main objectives in this study were to explore fronto-cerebellar connectivity using fcMRI and to provide a preliminary map of the resulting topography. The results identify patterns of correlated activity consistent with the principles derived from the foundational tract-tracing work on this subject (Middleton and Strick 1994; Kelly and Strick 2003). The results suggest that

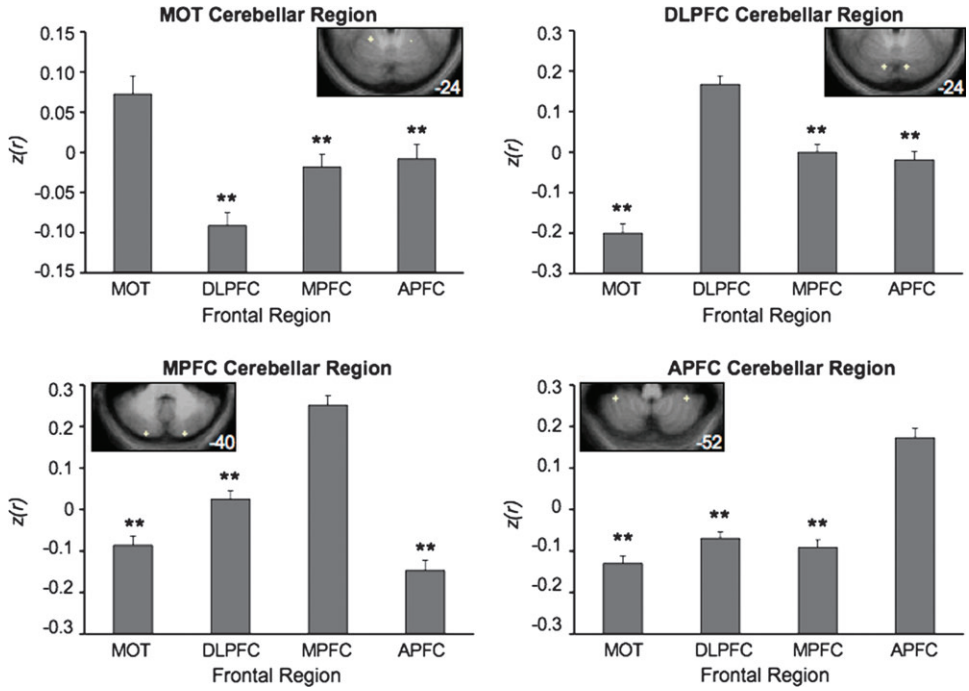

Figure 9. Fronto-cerebellar circuits dissociate in an independent data set. Spherical seed regions of 2-mm radius were drawn around local maxima in the cerebellar maps generated from Data Set 1. These regions were then carried forward and tested in the independent Data Set 2 to formally quantify the dissociation between the 4 fronto-cerebellar circuits. Each graph depicts the mean $z(r)$ between a given (bilateral) cerebellar region and each of the 4 bilateral frontal target regions. The cerebellar seed regions are depicted in the insets on each graph (coordinates: MOT cerebellar region: ±20, −50, −24; DLPFC cerebellar region: ±12, −80, −24; MPFC cerebellar region: ±22, −86, −40; APFC cerebellar region: ±36, −46, −52). $^{**}P < 0.001$.

fcMRI is constrained by anatomy and that it detects polysynaptic connectivity between regions. Moreover, although we present functional topography from 4 distinct regions in frontal cortex, viral tracing techniques have also identified widespread cerebellar projections to other association cortices including parietal cortex (Clower et al. 2001); clearly a great deal of cerebro-cerebellar connectivity remains to be explored. Direct comparisons with other primates may also be useful; for instance, in *Cebus* monkeys, ventral area 46 and lateral area 12 in prefrontal cortex do not appear to be anatomically connected with the cerebellum (Middleton and Strick 2001). Whether homologous areas in humans would also lack functional connectivity with the cerebellum is an open empirical question. Our provisional results suggest the intriguing possibility that the prefrontal cortex in humans is functionally coupled with a considerable extent of the cerebellum.

Supplementary Material

Supplementary material can be found at http://www.cercor.oxfordjournals.org/.

Funding

National Institute on Aging (AG-021910); Howard Hughes Medical Institute; Department of Defense (NDSEG fellowship to F.M.K.); Ashford Fellowship (to F.M.K.)

Notes

We thank Avi Snyder and Tanveer Talukdar for development of the fcMRI processing stream and Jeremy Schmahmann for discussion. *Conflict of interest*: None declared.

Address correspondence to email: krienen@wjh.harvard.edu.

References

Akkal D, Dum RP, Strick PL. 2007. Supplementary motor area and presupplementary motor area: targets of basal ganglia and cerebellar output. J Neurosci. 27(40):10659–10673.

Allen G, Buxton RB, Wong EC, Courchesne E. 1997. Attentional activation of the cerebellum independent of motor involvement. Science. 275(5308):1940–1943.

Allen G, McColl R, Barnard H, Ringe WK, Fleckenstein J, Cullum CM. 2005. Magnetic resonance imaging of cerebellar-prefrontal and cerebellar-parietal functional connectivity. Neuroimage. 28(1): 39–48.

Birn RM, Diamond JB, Smith MA, Bandettini PA. 2006. Separating respiratory-variation-related fluctuations from neuronal-activity-related fluctuations in fMRI. NeuroImage. 31(4):1536–1548.

Biswal B, Yetkin FZ, Haughton VM, Hyde JS. 1995. Functional connectivity in the motor cortex of resting human brain using echo-planar MRI. Magn Reson Med. 34(4):537–541.

Brainard DH. 1997. The psychophysics toolbox. Spat Vis. 10(4): 433–436.

Buckner RL, Andrews-Hanna JR, Schacter DL. 2008. The brain's default network: anatomy, function, and relevance to disease. Ann NY Acad Sci. 1124:1–38.

Buckner RL, Carroll DC. 2007. Self-projection and the brain. Trends Cogn Sci. 11(2):49–57.

Buckner RL, Sepulcre J, Talukdar T, Krienen FM, Liu H, Hedden T, Andrews-Hanna JR, Sperling R, Johnson KA. 2009. Cortical hubs revealed by intrinsic functional connectivity: mapping, assessment of stability, and relation to Alzheimer's disease. J Neurosci. 29(6): 1860–1873.

Clower DM, West RA, Lynch JC, Strick PL. 2001. The inferior parietal lobule is the target of output from the superior colliculus, hippocampus, and cerebellum. J Neurosci. 21(16):6283–6291.

De Luca M, Beckmann CF, De Stefano N, Matthews PM, Smith SM. 2006. fMRI resting state networks define distinct modes of long-distance interactions in the human brain. NeuroImage. 29(4): 1359–1367.

Desmond JE, Fiez JA. 1998. Neuroimaging studies of the cerebellum: language, learning and memory. Trends Cogn Sci. 2(9):355–362.
Dosenbach NUF, Fair DA, Miezin FM, Cohen AL, Wenger KK, Dosenbach RAT, Fox MD, Snyder AZ, Vincent JL, Raichle ME, et al. 2007. Distinct brain networks for adaptive and stable task control in humans. Proc Natl Acad Sci USA. 104(26):11073–11078.
Dum RP, Strick PL. 2003. An unfolded map of the cerebellar dentate nucleus and its projections to the cerebral cortex. J Neurophysiol. 89(1):634–639.
Evans AC, Collins DL, Mills SR, Brown ED, Kelly RL, Peters TE. 1993. 3D statistical neuroanatomical models from 305 MRI volumes. Paper presented at the Proc. IEEE-Nuclear Science Symposium and Medical Imaging Conference.
Fiez JA, Petersen SE, Cheney MK, Raichle ME. 1992. Impaired nonmotor learning and error-detection associated with cerebellar damage: a single case-study. Brain. 115:155–178.
Fox MD, Corbetta M, Snyder AZ, Vincent JL, Raichle ME. 2006. Spontaneous neuronal activity distinguishes human dorsal and ventral attention systems. Proc Natl Acad Sci USA. 103(26): 10046–10051.
Fox MD, Raichle ME. 2007. Spontaneous fluctuations in brain activity observed with functional magnetic resonance imaging. Nat Rev Neurosci. 8(9):700–711.
Fox MD, Snyder AZ, Vincent JL, Corbetta M, Van Essen DC, Raichle ME. 2005. The human brain is intrinsically organized into dynamic, anticorrelated functional networks. Proc Natl Acad Sci USA. 102(27):9673–9678.
Fransson P. 2005. Spontaneous low-frequency bold signal fluctuations: an fMRI investigation of the resting-state default mode of brain function hypothesis. Hum Brain Mapp. 26(1):15–29.
Greicius MD, Krasnow B, Reiss AL, Menon V. 2003. Functional connectivity in the resting brain: a network analysis of the default mode hypothesis. Proc Natl Acad Sci USA. 100(1):253–258.
Greicius MD, Supekar K, Menon V, Dougherty RF. 2009. Resting-state functional connectivity reflects structural connectivity in the default mode network. Cereb Cortex. 19(1):72–78.
Grodd W, Hülsmann ML, Wildgruber D, Erb M. 2001. Sensorimotor mapping of the human cerebellum: fMRI evidence of somatotopic organization. Hum Brain Mapp. 13(2):55–73.
Gusnard DA, Akbudak E, Shulman GL, Raichle ME. 2001. Medial prefrontal cortex and self-referential mental activity: relation to a default mode of brain function. Proc Natl Acad Sci USA. 98(7):4259–4264.
Gusnard DA, Raichle ME. 2001. Searching for a baseline: functional imaging and the resting human brain. Nat Rev Neurosci. 2(10): 685–694.
Honey CJ, Sporns O, Cammoun L, Gigandet X, Meuli R, Hagmann P. 2009. Predicting human resting state functional connectivity from structural connectivity. Proc Natl Acad Sci USA. 106(6): 2035–2040.
Huffman RF, Henson OW. 1990. The descending auditory pathway and acousticomotor systems: connections with the inferior colliculus. Bran Res Rev. 15(3):295–323.
Johnston JM, Vaishnavi SN, Smyth MD, Zhang DY, He BJ, Zempel JM, Shimony JS, Snyder AZ, Raichle ME. 2008. Loss of resting interhemispheric functional connectivity after complete section of the corpus callosum. J Neurosci. 28(25):6453–6458.
Kahn I, Andrews-Hanna JR, Vincent JL, Snyder AZ, Buckner RL. 2008. Distinct cortical anatomy linked to subregions of the medial temporal lobe revealed by intrinsic functional connectivity. J Neurophysiol. 100(1):129–139.
Kelly RM, Strick PL. 2003. Cerebellar loops with motor cortex and prefrontal cortex of a nonhuman primate. J Neurosci. 23(23): 8432–8444.
Leiner HC, Leiner AL, Dow RS. 1986. Does the cerebellum contribute to mental skills. Behav Neurosci. 100(4):443–454.
Leiner HC, Leiner AL, Dow RS. 1991. The human cerebrocerebellar system: its computing, cognitive, and language-skills. Behav Brain Res. 44(2):113–128.
Leiner HC, Leiner AL, Dow RS. 1993. Cognitive and language functions of the human cerebellum. Trends Cogn Sci. 16(11):444–447.
MacLeod CE, Zilles K, Schleicher A, Rilling JK, Gibson KR. 2003. Expansion of the neocerebellum in hominoidea. J Hum Evol. 44(4):401–429.
Margulies DS, Kelly AMC, Uddin LQ, Biswal BB, Castellanos FX, Milham MP. 2007. Mapping the functional connectivity of anterior cingulate cortex. Neuroimage. 37(2):579–588.
Matano S. 2001. Brief communication: proportions of the ventral half of the cerebellar dentate nucleus in humans and great apes. Am J Phys Anthropol. 114(2):163–165.
Matano S, Hirasaki E. 1997. Volumetric comparisons in the cerebellar complex of anthropoids, with special reference to locomotor types. Am J Phys Anthropol. 103(2):173–183.
Middleton FA, Strick PL. 1994. Anatomical evidence for cerebellar and basal ganglia involvement in higher cognitive function. Science. 266(5184):458–461.
Middleton FA, Strick PL. 2000. Basal ganglia and cerebellar loops: motor and cognitive circuits. Brain Res Rev. 31(2–3):236–250.
Middleton FA, Strick PL. 2001. Cerebellar projections to the prefrontal cortex of the primate. J Neurosci. 21(2):700–712.
O'Reilly JX, Mesulam MM, Nobre AC. 2008. The cerebellum predicts the timing of perceptual events. J Neurosci. 28(9): 2252–2260.
Petersen SE, Fox PT, Posner MI, Mintun M, Raichle ME. 1989. Positron emission tomographic studies of the processing of single words. J Cogn Neurosci. 1(2):153–170.
Raichle ME, MacLeod AM, Snyder AZ, Powers WJ, Gusnard DA, Shulman GL. 2001. A default mode of brain function. Proc Natl Acad Sci USA. 98(2):676–682.
Ramnani N, Behrens TEJ, Johansen-Berg H, Richter MC, Pinsk MA, Andersson JLR, Rudebeck P, Ciccarelli O, Richter W, Thompson AJ, et al. 2006. The evolution of prefrontal inputs to the cortico-pontine system: diffusion imaging evidence from macaque and humans. Cereb Cortex. 16(6):811–818.
Ravizza SM, McCormick CA, Schlerf JE, Justus T, Ivry RB, Fiez JA. 2006. Cerebellar damage produces selective deficits in verbal working memory. Brain. 129:306–320.
Rilling JK, Insel TR. 1998. Evolution of the cerebellum in primates: differences in relative volume among monkeys, apes and humans. Brain Behav Evol. 52(6):308–314.
Schmahmann JD. 1991. An emerging concept—the cerebellar contribution to higher function. Arch Neurol. 48(11):1178–1187.
Schmahmann JD. 1996. From movement to thought: anatomic substrates of the cerebellar contribution to cognitive processing. Hum Brain Mapp. 4(3):174–198.
Schmahmann JD. 2004. Disorders of the cerebellum: ataxia, dysmetria of thought, and the cerebellar cognitive affective syndrome. J Neuropsychiatry Clin Neurosci. 16(3):367–378.
Schmahmann JD. 2007a. The primary motor cerebellum is in the anterior lobe but not the posterior lobe. Evidence from stroke patients. Neurology. 68(12):A357.
Schmahmann JD. 2007b. Cerebellum and spinal cord: principles of development, anatomical organization, and functional relevance. In: Brice A, Pulst S, editors. Spinocerebellar degenerations: the ataxias and spastic paraplegias. New York: Elsevier. p. 1–60.
Schmahmann JD, Doyon J, McDonald D, Holmes C, Lavoie K, Hurwitz AS, Kabani N, Toga A, Evans A, Petrides M. 1999. Three-dimensional MRI atlas of the human cerebellum in proportional stereotaxic space. NeuroImage. 10:233–260.
Schmahmann JD, Doyon J, Toga A, Evans A, Petrides M. 2000. MRI atlas of the human cerebellum. San Diego (CA): Academic Press.
Schmahmann JD, Pandya DN. 1991. Projections to the basis pontis from the superior temporal sulcus and superior temporal region in the rhesus monkey. J Comp Neurol. 308(2):224–248.
Schmahmann JD, Pandya DN. 1993. Prelunate, occipitotemporal, and parahippocampal projections to the basis pontis in rhesus monkey. J Comp Neuro. 337(1):94–112.
Schmahmann JD, Pandya DN. 1997. Anatomic organization of the basilar pontine projections from prefrontal cortices in rhesus monkey. J Neurosci. 17(1):438–458.
Schmahmann JD, Pandya DN. 2008. Disconnection syndromes of basal ganglia, thalamus, and cerebrocerebellar systems. Cortex. 44(8): 1037–1066.

Schmahmann JD, Weilburg JB, Sherman JC. 2007. The neuropsychiatry of the cerebellum: insights from the clinic. Cerebellum. 6(3): 254–267.
Snider RS, Eldred E. 1951. Cerebro-cerebellar relationships in the monkey. J Neurophysiol. 15(27):27–40.
Spreng RN, Mar R, Kim ASN. 2009. The common neural basis of autobiographical memory, prospection, navigation, theory of mind and the default mode: a quantitative meta-analysis. J Cogn Neurosci. 21(3):489–510.
Stoodley CJ, Schmahmann JD. 2009. Functional topography in the human cerebellum: a meta-analysis of neuroimaging studies. NeuroImage. 44(2):489–501.
Svoboda E, McKinnon MC, Levine B. 2006. The functional neuroanatomy of autobiographical memory: a meta-analysis. Neuropsychologia. 44(12):2189–2208.
Van Dijk KRA, Hedden T, Tu PT, Laviolette P, Sperling RA, Buckner RL. 2008. Optimal acquisition parameters for resting state functional connectivity MRI. Society for Neuroscience Abstracts. 885.24.
Van Essen DC. 2005. A population-average, landmark- and surface-based (PALS) atlas of human cerebral cortex. NeuroImage. 28(3):635–662.
Vincent JL, Kahn I, Snyder AZ, Raichle ME, Buckner RL. 2008. Evidence for a frontoparietal control system revealed by intrinsic functional connectivity. J Neurophysiol. 100:3328–3342.
Vincent JL, Patel GH, Fox MD, Snyder AZ, Baker JT, Van Essen DC, Zempel JM, Snyder LH, Corbetta M, Raichle ME. 2007. Intrinsic functional architecture in the anaesthetized monkey brain. Nature. 447(7140):83–U84.
Vincent JL, Snyder AZ, Fox MD, Shannon BJ, Andrews JR, Raichle ME, Buckner RL. 2006. Coherent spontaneous activity identifies a hippocampal-parietal memory network. J Neurophysiol. 96(6): 3517–3531.
Whiting BA, Barton RA. 2003. The evolution of the cortico-cerebellar complex in primates: anatomical connections predict patterns of correlated evolution. J Hum Evol. 44(1):3–10.
Wise RG, Ide K, Poulin MJ, Tracey I. 2004. Resting fluctuations in arterial carbon dioxide induce significant low frequency variations in bold signal. NeuroImage. 21(4):1652–1664.
Zhang D, Snyder AZ, Fox MD, Sansbury MW, Shimony JS, Raichle ME. 2008. Intrinsic functional relations between human cerebral cortex and thalamus. J Neurophysiol. 100:1740–1748.